Oceanic swarms of Antarctic krill perform satiation sinking

Geraint A. Tarling, Sally E. Thorpe

British Antarctic Survey, Natural Environment Research Council, High Cross, Madingley Rd, Cambridge, CB3 0ET, UK

Abstract

Antarctic krill form some of the highest concentrations of animal biomass observed in the world's ocean potentially due to their prolific ability to swarm. Determining the movement of Antarctic krill within swarms is important to identify drivers of their behaviour and their biogeochemical impact on their environment. We examined vertical velocity within approximately 2000 krill swarms through the combined use of a shipborne echosounder and an acoustic Doppler current profiler (ADCP). We revealed a pronounced downward anomaly in vertical velocity within swarms of -0.6 $cm.s^{-1}$ compared with vertical motion outside the swarm. The anomaly changed over the diel cycle, with smaller downward anomalies occurring at night. Swarms in regions of high phytoplankton concentrations (a proxy for food availability) also exhibited significantly smaller downward anomalies. We propose that the anomaly is the result of downward velocities generated by the action of krill beating their swimming appendages. During the night and in high phytoplankton availability, when krill are more likely to feed to the point of satiation, swimming activity is lowered and the anomaly is reduced. Our findings are consistent with laboratory work where krill ceased swimming and adopted a parachute posture when sated. Satiation sinking behaviour can substantially increase the efficiency of carbon transport to depth through depositing faecal pellets at the bottom of swarms, avoiding the reingestion and breakup of pellets by other swarm members.

Keywords: Euphausia superba, acoustic Doppler current profiler, Southern Ocean, faecal pellets, carbon flux

Background

Swarming is a common behavioural trait in pelagic marine organisms that can improve fitness through reducing predation and increasing foraging success [1]. Swarms of Antarctic krill form some of the highest concentrations of animal biomass observed in the world's ocean, reaching densities of up to 2 Mt over an area of 100 km^2 [2]. Krill swarms have been observed in a wide range of configurations such as small compact aggregations (10–100 m long, 2–20 m thick [3]), extensive layers (41 km long [4]), superswarms [2], and dispersed formations throughout the water column [5]. The prolific ability of Antarctic krill to swarm may be a major factor in these organisms achieving arguably the highest monospecific biomass of any free-living animal on Earth (200 to 400 Mt [6]).

Advances in remote sensing and rapid data processing of underway cruise data are achieving unprecedented insights into the biomass distribution of krill swarms [7]. However, our understanding of how krill organise themselves and behave within swarms has not progressed to the same degree because of a lack of *in situ* observations, particularly in more open ocean environments [8]. Our best insights into within swarm behaviour are presently from laboratory based methods which have revealed the mechanisms of individual krill swimming. For instance, Murphy et al. [9] showed that krill swim through a metachronal beating of the pleopods (abdominal swimming appendages). Catton et al. [10] visualised the flow fields generated by free-swimming krill, which were generally downward and of the order of -1 to -4 cm s^{-1} over a distance of around 4 cm below the krill. This pattern was similar whether the krill were measured singularly or within small coordinated groups. Tarling and Johnson [11] showed that krill may not continuously swim, but alter between periods when the pleopods

beat continuously and cease beating altogether. During beat cessation, the pleopods are splayed out as if to control descent, which corresponds to the parachute mode captured by U. Kils using underwater photography of krill *in situ* (http://www.ecoscope.com). This parachute mode was found to occur more frequently in krill with full stomachs compared to those with empty stomachs [11]. Krill with fuller stomachs also beat their pleopods at a lower frequency and with decreased strength [12]. This suggests that krill undergo satiation sinking, where they descend during periods of digestion to reascend to the surface layers to feed when digestion is complete [13].

One potential means of examining behaviour within swarms is through acoustic Doppler current profilers (ADCPs), which measure Doppler shift in particles, principally as a means of measuring water velocity and direction. The instrument makes its calculations based on the assumption that all ensonified particles move passively [14] but this assumption may be violated if particles within any ensonifed layers are dominated by directionally swimming organisms. For instance, Wilson and Firing [15] found that residuals from tidal fits to ADCP data were conspicuously large at sunrise which they considered to be a bias from coherent horizontal swimming of dominant acoustic targets. Demer et al. [16] and Tarling and Thorpe [17] utilised this bias to measure the horizontal direction and velocity of fish schools and krill swarms respectively. ADCPs can also measure currents in the vertical dimension. Vertical currents are generally an order of magnitude lower than horizontal currents and any substantial vertical movements resolved by ADCPs are frequently attributed to the vertical migrations of pelagic organisms [18].

In this study, we measure instantaneous vertical velocities within krill swarms across the Scotia Sea (Southern Ocean) using acoustic information obtained through a combination of a ship-borne ADCP and a multifrequency EK60 echosounder. Our objectives are twofold, firstly to discern what identifiable effects krill swarms have on measured vertical flows

within the water column and, secondly, whether variability in these flows can provide insights into factors affecting the internal organisation of krill swarms. In particular, although krill swarms have been documented to undertake diel vertical migration, it is notably variable and even absent in certain instances [19]. Given that some swarms have vertical extents that can span much of the surface mixed layer, there remains the possibility that diel patterns of behaviour exist within the swarms themselves. Furthermore, the substantial thicknesses of many swarms (between 20 and 40 m [20]) means that not all individuals will be within the layer of greatest food concentration at any one time, suggesting that satiation sinking may be an important mechanism of positional turnover within swarms. Obtaining evidence of such behavioural traits will advance our understanding of how krill swarms operate and their sensitivity to prevailing environmental conditions.

Methods

Data were analysed from a survey carried out by the *RRS James Clark Ross* between 09 January and 16 February 2003 within the Scotia Sea sector of the Southern Ocean. Survey transects were transited at speeds of 9–18 km h^{-1} and covered approximately 13000 km (Fig S1 Electronic Supplementary Material). Acoustic data were collected using a combination of a calibrated Simrad split-beam EK60 echosounder with 38 kHz and 120 kHz transducers and an RD Instruments narrow-band 153.6 kHz ship-mounted ADCP (full details on the configurations of the acoustic instruments and data matching procedures are given in Electronic Supplementary Material). Net deployments were made intermittently along the transects from which krill population structure was determined and used for the parameterization of target identification models. Swarms that were detected within 100 km of any coastline were excluded from the analysis to ensure that the study only considered the open-ocean situation, given that krill adopt different behavioural strategies in more inshore regions [21]. A vertical velocity anomaly (w_{net}, cm s^{-1}) was determined for each swarm where

there was a valid estimate of ADCP derived vertical velocity both within the swarm (w_{obs}) and outside the swarm (i.e. above and/or below the swarm, w_{pre}, Dataset S1). w_{obs} was taken to be the vertical velocity from the single ADCP bin corresponding to the mid-depth and mid-length point of the swarm. To determine vertical velocity outside the swarm, the closest bin above and below the swarm's vertical extent at the mid-length point of the swarm was chosen since this allowed all sizes of swarms to be measured on a similar basis. In total, w_{net} was derived for a total of 2043 swarms. The same procedure was followed in a further analysis to identify any artefacts in the w_{net} calculation method and to derive a baseline level of w_{net} to which the influence of krill swarms could be compared. This analysis drew "fake" swarms of similar dimensions to observed swarms (Table S1) in swarm devoid regions and determined w_{net} as above (see Electronic Supplementary Material). The effect of light on swarm behaviour was tested through matching observed swarms with photosynthetically active radiation (PAR), measured by a parlite quantum sensor (Kipp and Zonen), which collected measurements at 5 s intervals, subsequently averaged into 1 min intervals. Phytoplankton availability for each swarm was derived through matching to the relevant spatial 4 x 4 km pixel of 8-day synthesised sea surface chlorophyll-a (Chl-a) images provided by the MODIS instrument on board the Aqua satellite (operated by NASA).

Results

Vertical velocity anomalies within krill swarms Our method compared the vertical velocities (w, cm s^{-1}) within the swarm to those immediately outside (both above and below the swarm) to derive a vertical velocity anomaly, w_{net} (Fig. 1). Vertical velocities inside and outside the swarms were significantly different, with median w_{net} being downwards at -0.61 cm s^{-1} (Mann-Whitney [MW] rank sum test, U=18740070, T = 3928016, n(small) = 2043, n(big) = 2043, P = <0.001). We verified that the pattern was not an artefact of the processing method through carrying out the same calculations in areas where there were no krill swarms (termed

125 "fake" swarms) for which we found there to be no significant difference between vertical
126 velocities outside of and within fake swarm regions (MW test, U = 4439200, T = 8880890,
127 n(small) = 2980, n(big) = 2980), P = 0.988, Fig. 2).

128 *Relationship to the diel cycle:* We found there to be a significant difference in w_{net} between
129 different phases of the diel cycle (Krusall-Wallis 1-way ANOVA, H = 29.98, 3 df, P<0.001,
130 Fig. 3). Individual significant differences were found between day and night (All pairwise
131 comparison, Dunns Method, difference in ranks 183.1, Q = 3.794), and between dawn and
132 day (Difference in ranks 327.4, Q = 3.757). All other comparisons did not show significant
133 differences. Daytime contained the lowest median value for w_{net} (-0.71 cm s^{-1}) with nighttime
134 and dusk also exhibiting negative (downward) median vertical velocity anomalies (both being
135 -0.10 cm s^{-1}). w_{net} was positive (upward) during dawn (0.51 cm s^{-1}). During the daytime, we
136 found no influence of different levels of daylight on w_{net} when comparing between low PAR
137 and high PAR situations (MW test, U = 199090, T = 379208, n(small) = 588, n(big) = 689, P
138 = 0.597).

139 *Relationship to surface Chl-a:* w_{net} was significantly more negative in regions with low levels
140 of surface Chl-a compared to regions where surface Chl-a was high, both when including all
141 times of day and night (MW test, U = 58654, T = 88409, n(small) = 149, n(big) = 912, P =
142 0.007) and when restricting the analysis to daytime only (MW test, U = 39204, T = 55969,
143 n(small) = 103, n(big) = 872, P = 0.035). Across all times of day and night, median w_{net} was -
144 0.81 cm s^{-1} in low Chl-a conditions compared to -0.25 cm s^{-1} when Chl-a was high (Fig. 4).

145

146 ## Discussion

147 *Vertical velocity anomalies within krill swarms* Through comparing vertical velocities within
148 and immediately outside of swarms, we determined there to be a downward velocity anomaly
149 within swarms of -0.6 cm s^{-1}. Such an anomaly did not exist over similar dimensions of the

water column where there were no krill swarms. Although it can be deduced that krill within swarms are responsible for the anomaly, it remains unclear how they produce it. One possibility is that it reflects the movement of the krill themselves within the body of the swarm. Alternatively, it may be generated by the movement they impart to the water through the beating of their pleopods, assuming that pleopod beating deflects small particles downwards, so generating a negative Doppler shift detectable by the ship-borne ADCP.

Although we do not have direct evidence on how the anomalies are generated within swarms, we can rule out certain explanations based on other available evidence. For instance, if the anomaly is produced by the movement of individuals within swarms, it implies that the average swarm must always be migrating downwards. Swarms are typically found within the top 100 m of the water column and maintain this relatively narrow vertical distribution over diel cycles [19]. Such a bias towards downward moving swarms would be contrary to our understanding of krill swarm distribution and behaviour. It is further possible that the downward anomaly may reflect an avoidance behaviour in krill with respect to the survey ship, as has been found in fish during trawling [22] [16]. However, there were no nets in the water during the acoustic observations included in the present analysis. Furthermore, w_{net} significantly varied according to time of day which rules out a response to ship's noise, which can be assumed to be relatively constant day and night. Another explanation is that krill may be responding to a shadowing of light by the vessel. The average depth of a swarm was 50 m below the vessel, by which depth light is not fully attenuated. We tested this possibility by comparing w_{net} between high and low PAR situations, assuming that any shadowing effect would have been more marked when PAR was high and found there to be no significant difference in w_{net} between these two light environments. Although some avoidance behaviour cannot be ruled out, it does not offer a consistent explanation for the patterns and cycles we observed in w_{net}.

In the case of the downward deflection of small particles through pleopod beating, it is necessary first to consider the swimming action of Antarctic krill. When swimming, Antarctic krill rely on a mix of both drag-based and momentum-based swimming [10]. Their body size and density means that they are negatively buoyant and must beat their pleopods continuously in order to maintain their position within the water column [23]. When hovering, the majority of the thrust required to maintain position is directed downwards [23]. This may be less the case when swimming forwards although a large downward component is still produced [10]. These downward velocities will collectively dominate the vertical velocity signal wherever the krill are resident in sufficiently high concentrations. Nevertheless, ADCPs do not resolve water movement directly but rely on detecting Doppler shift in particles that are assumed to represent water movement. Within krill swarms, likely candidates of such particles are the background zooplankton communities and suspended particulate matter, as were also resolved in "fake" swarm regions (areas devoid of swarms that were used as controls). A further matter is that ADCPs average all velocities within respective depth-time bins, which will modulate the influence of specific sources such as the wakes of swimming krill. This therefore may explain why our observed anomaly of -0.6 cm s^{-1} is below the range expected in terms of the downward water movements imparted by swarming Antarctic krill, which are of the order of -1 to -4 cm s^{-1} [10].

Diel periodicity in anomalies We found that the downward vertical velocity anomaly was significantly greater during the daytime than in other phases of the 24 h cycle. The downward anomaly was around -0.7 cm s^{-1} during the day compared to around -0.1 cm s^{-1} during dusk and nighttime. The diel change in this anomaly implies that the swimming behaviour of individuals within the swarm must also be altering on a diel basis. Assuming that the anomaly is the result of the downward velocity imparted to the water by krill pleopod beating, it follows that either the power or the duration of these beats decreases during the night.

In free running dark and light:dark incubations, Gaten et al. [24] found that krill have complex diel rhythms in swimming behaviour made of two circadian components, one shorter than 24 h and one longer than 24 h, to which is added a further 12 h rhythmic component. Godlewska [19] also identified a 24 h and 12 h component in the diel vertical migration patterns of Antarctic krill derived from acoustic and net sample analyses. We propose that one manifestation of this behavioural periodicity are phases of stronger and weaker pleopod beating over the course of the day-night cycle.

One interesting observation was the positive anomaly of 0.5 cm s^{-1} observed at dawn. Krill during this survey were observed to undertake a reverse vertical migration from 80 m during the night to 40 m during the day (Tarling, pers. obs). The positive anomaly may be the one instance where the upward movement of the krill themselves dominates the ADCP estimate of vertical velocity. Such upward anomalies are consistent with ADCP observations of other swarming euphausiid species during upward migration phases [25].

Satiation sinking in krill swarms Our further finding was that downward velocities were significantly lower in high phytoplankton food environments (for which surface Chl-a was used as a proxy). This suggests that the process of feeding also has implications on krill swimming behaviour. At an individual level, laboratory-based tethering experiments have shown that satiation in krill can cause a decrease in swimming activity and the adoption of a parachute posture which may facilitate periods of controlled sinking [11, 12]. In the natural environment, this implies that swarms within regions of high food availability will be more likely to contain individuals undergoing satiation sinking. In this scenario, a fraction of the krill population stops beating and outsplays their pleopods when their stomachs are full. This means that they will no longer contribute to the generation of downward velocities. The result is a decrease in the overall downward anomaly. It follows that downward anomalies are likely to be smaller in rich feeding environments where satiation is more likely to occur.

Given that sinking individuals must be replaced by other upwardly swimming individuals if the swarm is to remain intact, there will be a continual vertical overturn of individuals within swarms found in food rich environments. This continual upward and downward movement of individuals will have an impact on swarm organisation, particularly inter-individual distances and packing concentrations. In a further analysis taken across all swarms identified during the present survey, we found that packing concentrations were significantly lower both during nighttime and in high food environments (MW test: night vs day, U = 101822, T= 115118 n(small) = 163, n(big) = 1802, P = <0.001; high vs low Chl-a, U = 43048, T = 54223, n(small) = 149, n(big) = 912, P = <0.001). When adopting the parachute posture in satiation sinking mode, krill no longer have the requirement to maintain optimal positions relative to their nearest neighbours, which will lead to swarm structure becoming less organised and more dispersed. Direct demonstrations in controlled conditions would be a logical next step to support this hypothesis.

Influence of swarms on vertical flows and mixing The vertical velocity anomaly that we observed within krill swarms implies that these swarms have a resolvable and significant impact on the velocities of the bodies of water they occupy. This supports the position of earlier studies considering the influence that krill swarms have on ocean mixing. Huntley and Zhou [26], for instance, calculated that swarms produce turbulent energy at a rate that is 3 to 4 orders of magnitude greater than the background average rate of turbulent energy dissipation. Kunze et al. [27] similarly found turbulence that was three to four orders of magnitude larger during the dusk ascent of a dense acoustic-scattering layer of krill compared to background levels during the day and that this elevated the daily-averaged mixing in the inlet by a factor of 100. Nevertheless, further studies have not found evidence of increased turbulence within aggregations of marine organisms or during periods of vertical migration [28, 29]. Although not universal, the impact of swarms and vertical migration on ocean

mixing may be significant in certain situations, particularly in the seasonally stratified layers and in coastal regions during summer, facilitating the upward mixing of limiting nutrients from depth [26, 27]. This may indeed be an important process in the continuation of large blooms that are major hotspots for krill [30].

Biogeochemical impact of satiation sinking One of the major consequences of the vertical movement of pelagic organisms is that they contribute to the transport of carbon and nitrogen from the food rich layers at the surface to the ocean interior, a process otherwise referred to as the 'biological pump' [31]. In the case of synchronised vertical migration, this would occur at dawn when organisms that had just fed at the surface migrate downwards and defecate, respire and excrete in the ocean interior [32]. This active transport of materials downwards avoids interception and break-up en-route which otherwise limits the efficiency of the passive process of dead matter and faeces sinking through gravity alone from the surface layers to depth. However, the fact that active transport from synchronised vertical migration occurs during just a short time window around dawn limits the overall contribution of this process to the biological pump. Under a scenario of satiation sinking within krill swarms, active transport will occur whenever there is sufficient food available for individuals to become sated and sink [13]. As well as short-circuiting the community of organisms that feed on detritus in the upper water column, this behaviour also ensures that a large fraction of faeces are egested towards the bottom of the krill swarm, so avoiding refiltering and interference by other swarm members.

Our proposal that satiation sinking is common within krill swarms is supported by observations showing that krill faecal pellets can dominate the material collected by deep sediment traps at many localities within the Southern Ocean [33-36]. In the present study region, Manno et al. [37] found that faecal pellets can make up 91% of total sedimentary particulate carbon, with around a fifth being derived from krill. Krill faecal pellets have also

been found to dominate sinking material further up the water column, in the region just below the surface mixed layer [38, 39]. Indeed, Belcher et al. [39] found krill faecal pellets were sometimes just as abundant below the surface mixed layer as within it, even though the majority of krill swarms themselves did not extend below the surface mixed layer, showing that faecal pellets can be exported from swarms very efficiently. This would not be the case if the majority of faecal pellets were generated randomly within swarms and had to pass through much of the swarm before being exported rather than be produced mostly towards the bottom of swarms as a result of satiation sinking. The contribution to the biological pump of satiation sinking within krill swarms can be substantial, potentially sequestering 23 Mt of carbon to the ocean interior each year within the Southern Ocean [11].

Conclusions

Our evidence shows that the presence of krill swarms produces a downward anomaly in the background level of vertical movement in the water column of -0.6 cm s^{-1}. Rather than being the result of the movement of individual krill within the swarm, we interpret this anomaly to be the product of the downward velocities generated by krill beating their pleopods continuously and so allowing them to overcome their negative buoyancy and remain pelagic. The downward anomaly was found to be significantly smaller during nighttime and in regions of high phytoplankton food availability (high Chl-a) when feeding levels are likely to be high. The latter result is congruent with the findings of laboratory experiments in which krill with full stomachs were more likely to cease beating and outsplay their pleopods in a phase of controlled sinking. The consistency between in situ observations and laboratory results indicates that satiation sinking is likely to be a common feature within krill swarms. Satiation sinking can increase the probability of faecal pellets remaining intact and sinking to depth. This may help to explain the high krill concentrations of krill faecal pellets found below the surface mixed layer and at bathypelagic depths within the Southern Ocean.

Acknowledgements: The crew and scientists aboard the RRS *James Clark Ross* during the cruise JR82, D. Bone for assembling and maintaining the net gear and N. Cunningham for organizing and retrieving data. S. Fielding and T. Klevjer assisted in the acoustic identification and visualisation of krill swarms, as reported in previously published works. A. Atkinson, D. Pond, and R. Shreeve helped with the morphometric measurement and maturity staging of Antarctic krill captured by nets during the cruise, and H. Venables gave advice on the ADCP data. MODIS chlorophyll data was provided by the NASA Ocean Biology Processing Group.

Funding: This work was funded by the Natural Environment Research Council, UK through its support of the Ecosystems program at the British Antarctic Survey.

Author contributions: GAT participated in the krill sampling expedition, carried out the statistical analysis on the acoustic data, developed the hypotheses and drafted the manuscript; SET participated in the krill sampling expedition, processed and matched the ADCP data to the krill acoustic data and contributed to manuscript writing. Both authors give final approval for publication.

Competing Interests: The authors declare that no competing interests exist.

References

[1] Foster, E.G., Ritz, D.A., Osborn, J.E. & Swadling, K.M. 2001 Schooling affects the feeding success of Australian salmon (*Arripis trutta*) when preying on mysid swarms (*Paramesopodopsis rufa*). *J. Exp. Mar. Biol. Ecol.* **261**, 93-106. (doi:10.1016/s0022-0981(01)00265-9).

[2] Nowacek, D.P., Friedlaender, A.S., Halpin, P.N., Hazen, E.L., Johnston, D.W., Read, A.J., Espinasse, B., Zhou, M. & Zhu, Y.W. 2011 Super-aggregations of krill and Humpback whales in Wilhelmina Bay, Antarctic Peninsula. *PLOS One* **6**. (doi:10.1371/journal.pone.0019173).

[3] Kalinowski, J. & Witek, Z. 1985 Scheme for classifying Antarctic krill. *BIOMASS Handbook Ser.* **27**, 1-12.

[4] Watkins, J.L. & Murray, A.W.A. 1998 Layers of Antarctic krill, *Euphausia superba*: are they just long krill swarms? *Mar. Biol.* **131**, 237-247. (doi:10.1007/s002270050316).

[5] Everson, I. 1982 Diurnal variations in mean volume backscattering strength of an Antarctic krill (*Euphausia superba*) patch. *J. Plankt. Res.* **4**, 155-162. (doi:10.1093/plankt/4.1.155).

[6] Atkinson, A., Siegel, V., Pakhomov, E.A., Rothery, P., Loeb, V., Ross, R.M., Quetin, L.B., Schmidt, K., Fretwell, P., Murphy, E.J., et al. 2008 Oceanic circumpolar habitats of Antarctic krill. *Mar. Ecol. Prog. Ser.* **362**, 1-23. (doi:10.3354/meps07498).

[7] Siegel, V. & Watkins, J.L. 2016 Distribution, biomass and demography of Antarctic krill, *Euphausia superba*. In *Biology and Ecology of Antarctic krill* (ed. V. Siegel), pp. 21-100. Switzerland, Springer International Publishing.

[8] Hamner, W.M. & Hamner, P.P. 2000 Behavior of Antarctic krill (*Euphausia superba*): schooling, foraging, and antipredatory behavior. *Can. J. Fish. Aquat. Sci.* **57**, 192-202. (doi:10.1139/cjfas-57-S3-192).

[9] Murphy, D.W., Webster, D.R., Kawaguchi, S., King, R. & Yen, J. 2009 Locomotory Biomechanics of Antarctic Krill. *Integr.Compar. Biol.* **49**, E121-E121.

[10] Catton, K.B., Webster, D.R., Kawaguchi, S. & Yen, J. 2011 The hydrodynamic disturbances of two species of krill: implications for aggregation structure. *J. Exp. Biol.* **214**, 1845-1856. (doi:10.1242/jeb.050997).

[11] Tarling, G.A. & Johnson, M.L. 2006 Satiation gives krill that sinking feeling. *Curr. Biol.* **16**, R83-R84. (doi:10.1016/j.cub.2006.01.044).

[12] Johnson, M.L. & Tarling, G.A. 2008 Influence of individual state on swimming capacity and behaviour of Antarctic krill. *Mar. Ecol. Prog. Ser.* **366**, 99-110. (doi:10.3354/meps07533).

[13] Pearre, S. 2003 Eat and run? The hunger/satiation hypothesis in vertical migration: history, evidence and consequences. *Biol. Rev.* **78**, 1-79. (doi:10.1017/S146479310200595X).

[14] Woodward, W.E. & Appell, G.F. 1986 Current velocity measurements using acoustic Doppler backscatter: a review. *IEEE J. ocean. Engng.* **OE-11**, 3-6.

[15] Wilson, C.D. & Firing, E. 1992 Sunrise swimmers bias acoustic Doppler current profiles. *Deep Sea Res.* **39**, 885-892. (doi:10.1016/0198-0149(92)90127-F).

[16] Demer, D.A., Barange, M. & Boyd, A.J. 2000 Measurements of three-dimensional fish school velocities with an acoustic Doppler current profiler. *Fish. Res.* **47**, 201-214. (doi:10.1016/s0165-7836(00)00170-3).

[17] Tarling, G.A. & Thorpe, S.E. 2014 Instantaneous movement of krill swarms in the Antarctic Circumpolar Current. *Limnol. Oceanogr.* **59**, 872-886. (doi:10.4319/lo.2014.59.3.0872).

[18] Pleuddemann, A.J. & Pinkel, R. 1989 Characterization of the patterns of diel migration using a Doppler sonar. *Deep-Sea Res.* **36**, 509-530. (doi:10.1016/0198-0149(89)90003-4).

[19] Godlewska, M. 1996 Vertical migrations of krill (*Euphausia superba* Dana). *Pol. Arch. Hydrobiol.* **14**, 9-63. (doi:10.1007/BF00297159).

[20] Tarling, G.A., Klevjer, T., Fielding, S., Watkins, J., Atkinson, A., Murphy, E., Korb, R., Whitehouse, M. & Leaper, R. 2009 Variability and predictability of Antarctic krill swarm structure. *Deep-Sea Res. Part II* **56**, 1994-2012. (doi:10.1016/j.dsr.2009.07.004).

[21] Klevjer, T.A., Tarling, G.A. & Fielding, S. 2010 Swarm characteristics of Antarctic krill Euphausia superba relative to the proximity of land during summer in the Scotia Sea. *Marine Ecology Progress Series* **409**, 157-170. (doi:10.3354/meps08602).

[22] Olsen, K. & Lovik, A. 1982 Observed fish reactions to a surveying vessel with special reference to herring, cod, capelin and polar cod. *Symp. Fish. Acoust., Bergen, Norway.* **48**, 21-24.

374 [23] Kils, U. 1981 Swimming behaviour, swimming performance and energy balance of Antarctic krill
375 *Euphausia superba*. *BIOMASS Scientific Ser.* **3**, pp. 1-121.
376 [24] Gaten, E., Tarling, G., Dowse, H., Kyriacou, C. & Rosato, E. 2008 Is vertical migration in Antarctic
377 krill (*Euphausia superba*) influenced by an underlying circadian rhythm? *J. Genet.* **87**, 473–483.
378 (doi:10.1007/s12041-008-0070-y).
379 [25] Tarling, G.A., Matthews, J.B.L., David, P., Guerin, O. & Buchholz, F. 2001 The swarm dynamics of
380 Northern krill (*Meganyctiphanes norvegica*) and pteropods (*Cavolinia inflexa*) during vertical
381 migration in the Ligurian Sea observed by an Acoustic Doppler Current Profiler. *Deep-Sea Res. Part I*
382 **48**, 1671-1686. (doi:10.1016/S0967-0637(00)00105-9).
383 [26] Huntley, M.E. & Zhou, M. 2004 Influence of animals on turbulence in the sea. *Mar. Ecol. Prog.*
384 *Ser.* **273**, 65-79. (doi:10.3354/meps273065).
385 [27] Kunze, E., Dower, J.F., Beveridge, I., Dewey, R. & Bartlett, K.P. 2006 Observations of biologically
386 generated turbulence in a coastal inlet. *Science* **313**, 1768-1770. (doi:10.1126/science.1129378).
387 [28] Gregg, M.C. & Horne, J.K. 2009 Turbulence, acoustic backscatter, and pelagic nekton in
388 Monterey Bay. *J. Phys. Oceanogr.* **39**, 1097-1114. (doi:10.1175/2008JPO4033.1).
389 [29] Rippeth, T., J.Gascoigne, J.Green, Inall, M., Palmer, M., Simpson, J. & Wiles, P. 2007 Turbulent
390 dissipation of coastal seas. *Science, E-letter* **[Available online at**
391 **http://www.sciencemag.org/cgi/eletters/313/5794/1768#10043.]**.
392 [30] Schmidt, K., Schlosser, C., Atkinson, A., Fielding, S., Venables, H.J., Waluda, C.M. & Achterberg,
393 E.P. 2016 Zooplankton gut passage mobilizes lithogenic iron for ocean productivity. *Curr. Biol.* **26**,
394 2667-2673. (doi:10.1016/j.cub.2016.07.058).
395 [31] Ducklow, H.W., Steinberg, D.K. & Buesseler, K.O. 2001 Upper ocean carbon export and the
396 biological pump. *Oceanography (Washington DC)* **14**, 50-58.
397 [32] Wallace, M.I., Cottier, F.R., Brierley, A.S. & Tarling, G.A. 2013 Modelling the influence of
398 copepod behaviour on faecal pellet export at high latitudes. *Polar Biol.* **36**, 579-592.
399 (doi:10.1007/s00300-013-1287-7).

400 [33] Dunbar, R. 1984 Sediment trap experiments on the Antarctic continental margin. *Antarct. J.*
401 *United States* **19**, 70-71.
402 [34] von Bodungen, B., Fischer, G., Nöthig, E.-M. & Wefer, G. 1987 Sedimentation of krill faeces
403 during spring development of phytoplankton in Bransfield Strait, Antarctica. *Mitt Geol Paläont Inst*
404 *Univ Hamburg, SCOPE/UNEP Sonderbd.* **62**, 243-257.
405 [35] Bathmann, U., Fischer, G., Müller, P. & Gerdes, D. 1991 Short-term variations in particulate
406 matter sedimentation off Kapp Norvegia, Weddell Sea, Antarctica: relation to water mass advection,
407 ice cover, plankton biomass and feeding activity. *Polar Biol.* **11**, 185-195. (doi:10.1007/BF00240207).
408 [36] Accornero, A., Manno, C., Esposito, F. & Gambi, M. 2003 The vertical flux of particulate matter
409 in the polynya of Terra Nova Bay. Part II. Biological components. *Antarct. Sci.* **15**, 175-188.
410 (doi:10.1017/S0954102003001214).
411 [37] Manno, C., Stowasser, G., Enderlein, P., Fielding, S. & Tarling, G.A. 2015 The contribution of
412 zooplankton faecal pellets to deep-carbon transport in the Scotia Sea (Southern Ocean).
413 *Biogeosciences* **12**, doi:10.5194/bg-5112-1955-2015.
414 [38] Cadée, G., González, H. & Schnack-Schiel, S. 1992 Krill diet affects faecal string settling. *Polar*
415 *Biol.* **12**, 75-80. (doi:10.1007/BF00238267).
416 [39] Belcher, A., Tarling, G., Manno, C., Atkinson, A., Ward, P., Skaret, G., Fielding, S., Henson, S. &
417 Sanders, R. 2017 The potential role of Antarctic krill faecal pellets in efficient carbon export at the
418 marginal ice zone of the South Orkney Islands in spring. *Polar Biol.*, 1-13. (doi:10.1007/s00300-017-
419 2118-z).

Figure legends

Fig. 1: Example of a krill swarm resolved by an EK60 echosounder. The krill swarm (yellow irregular object) was observed on 27th January 2003 at 58.80°S, 41.69°W. ADCP vertical velocities are superimposed (boxes and arrows; cm s^{-1}). The green box denotes the mid-swarm vertical velocity w_{obs} while the orange boxes are values above and below the limits of the swarm, which are averaged to determine w_{pre}. Vertical velocity anomaly (w_{net}) represents w_{obs} minus w_{pres} which is -3.85 cm s^{-1} in the present example, representing a downward anomaly.

Fig. 2: Comparison of vertical velocities (w) measured inside and immediately outside of krill swarms. Refer to Fig. 1 for illustration of ADCP bin selection. Measurements for outside of swarm represent the average of the closest bins above and below the swarm's vertical extent at the mid-length point of the swarm. Notched horizontal line represents the median, limits of boxes, the 25th and 75th percentiles, and vertical lines, 1.5 times the interquartile range.

Fig 3: Downward vertical velocity anomaly (w_{net}) at different phases of the diel cycle. A positive value for w_{net} represents an upward anomaly, a negative value, a downward anomaly. Notched horizontal line represents the median, limits of boxes, the 25th and 75th percentiles, and vertical lines, 1.5 times the interquartile range.

Fig 4: Downward vertical velocity anomaly (w_{net}) in high versus low Chl-a. High Chl-a was defined as being values ≥0.5 mg m^{-3}, and low values, <0.5 mg m^{-3}. A positive value for w_{net} represents an upward anomaly, a negative value, a downward anomaly. Notched horizontal

443 line represents the median, limits of boxes, the 25th and 75th percentiles, and vertical lines, 1.5

444 times the interquartile range.

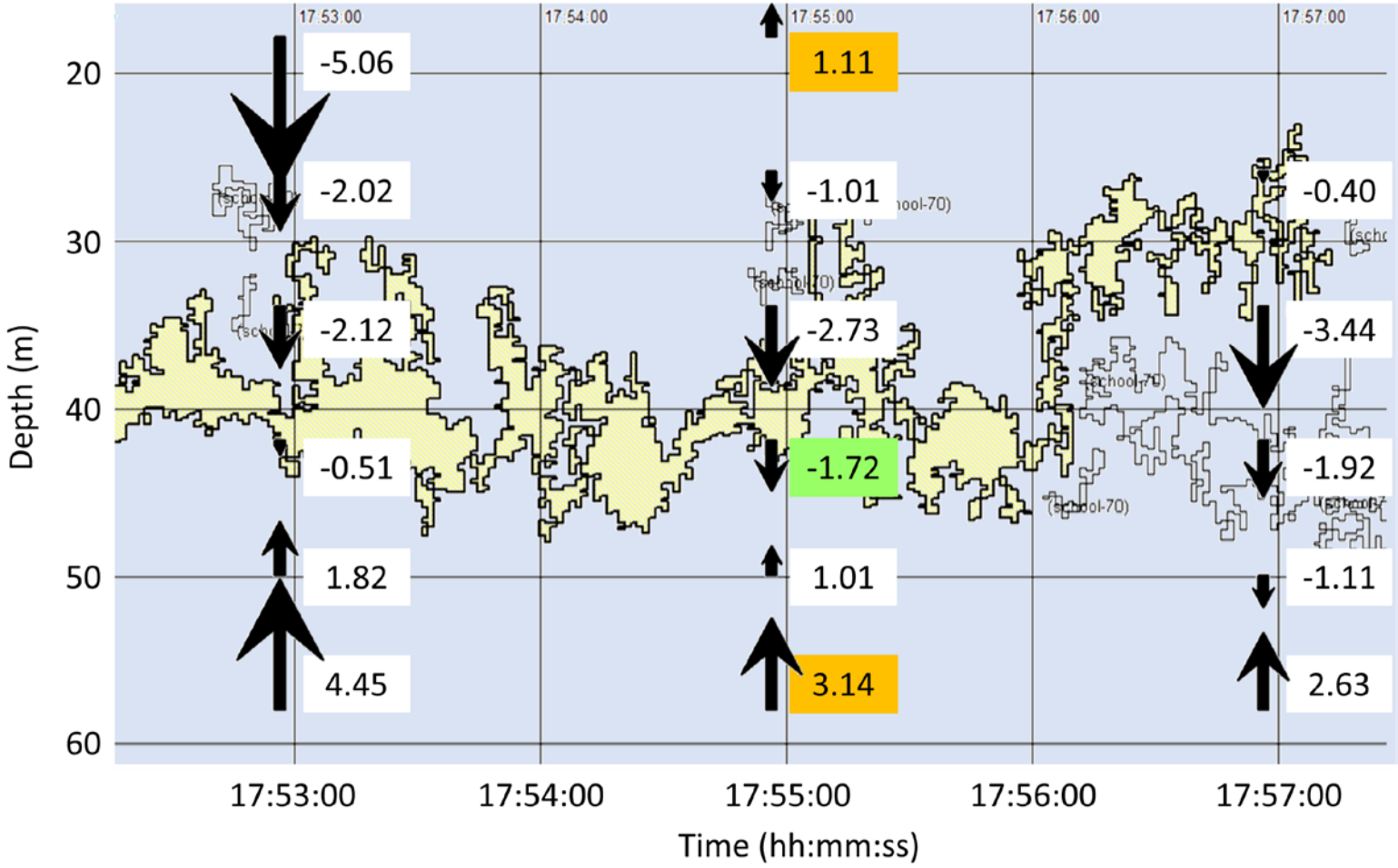
17:53:00
17:54:00
17:55:00
17:56:00
17:57:00
-5.06
-2.02
-2.12
-0.51
1.82
4.45
1.11
-1.01
-2.73
-1.72
1.01
3.14
-0.40
-3.44
-1.92
-1.11
2.63
20
30
40
50
60
Depth (m)
17:53:00
17:54:00
17:55:00
17:56:00
17:57:00
Time (hh:mm:ss)

Fig. 1

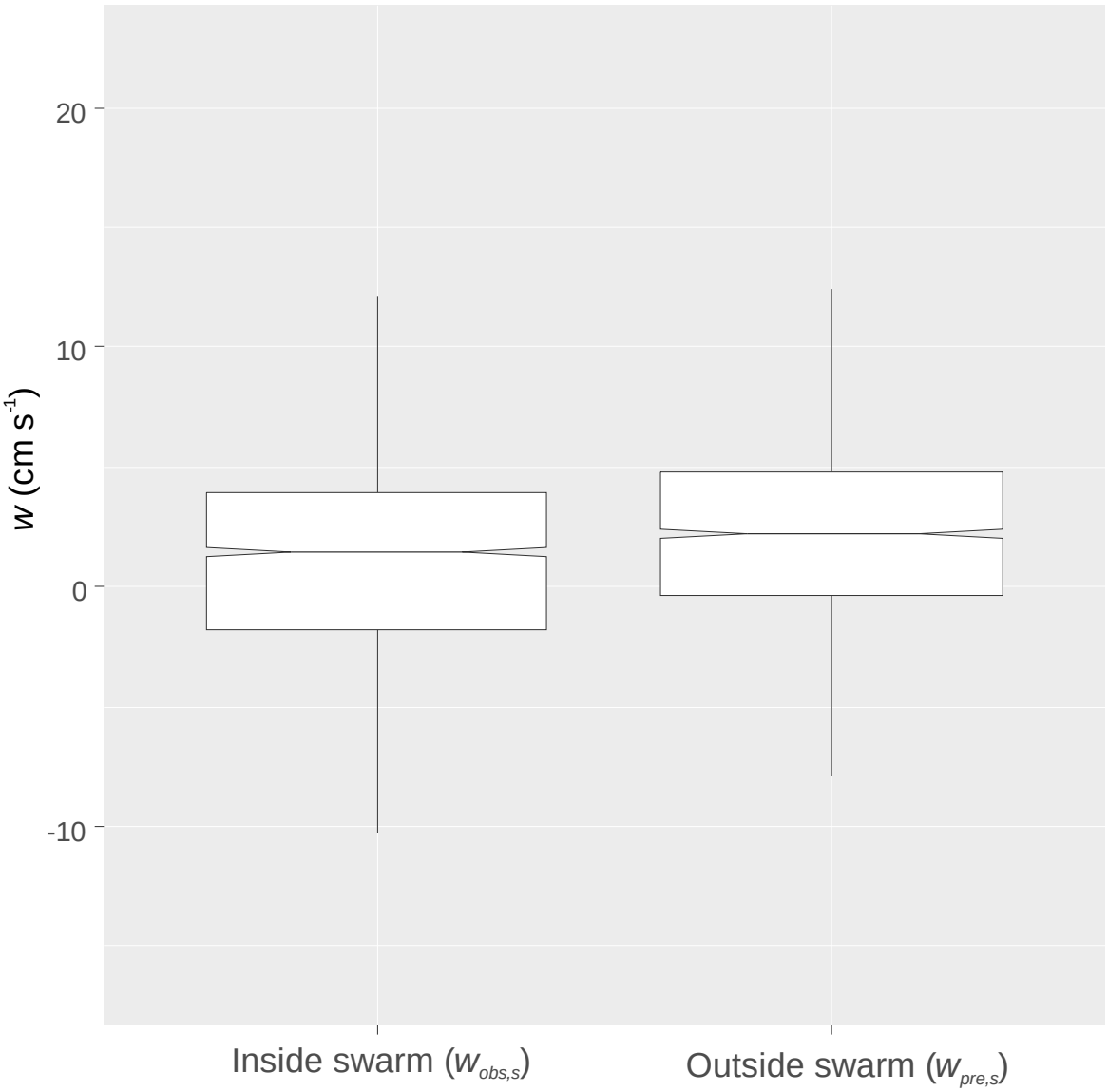
20
10
0
-10
w (cm s-1)
Inside swarm (wobs,s)
Outside swarm (wpre,s)

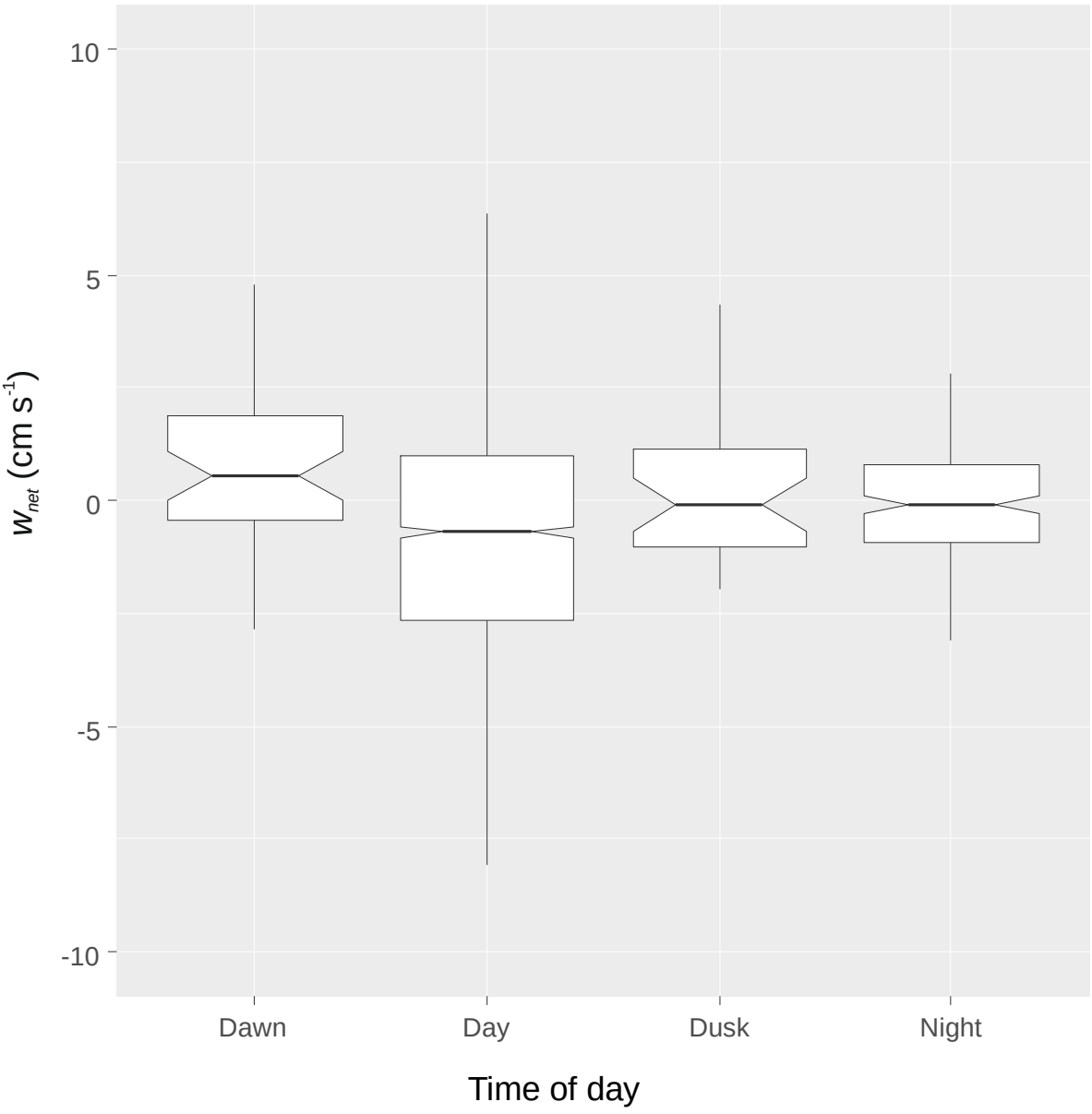
10
5
0
-5
-10
w_{net} (cm s^{-1})
Dawn
Day
Dusk
Night
Time of day

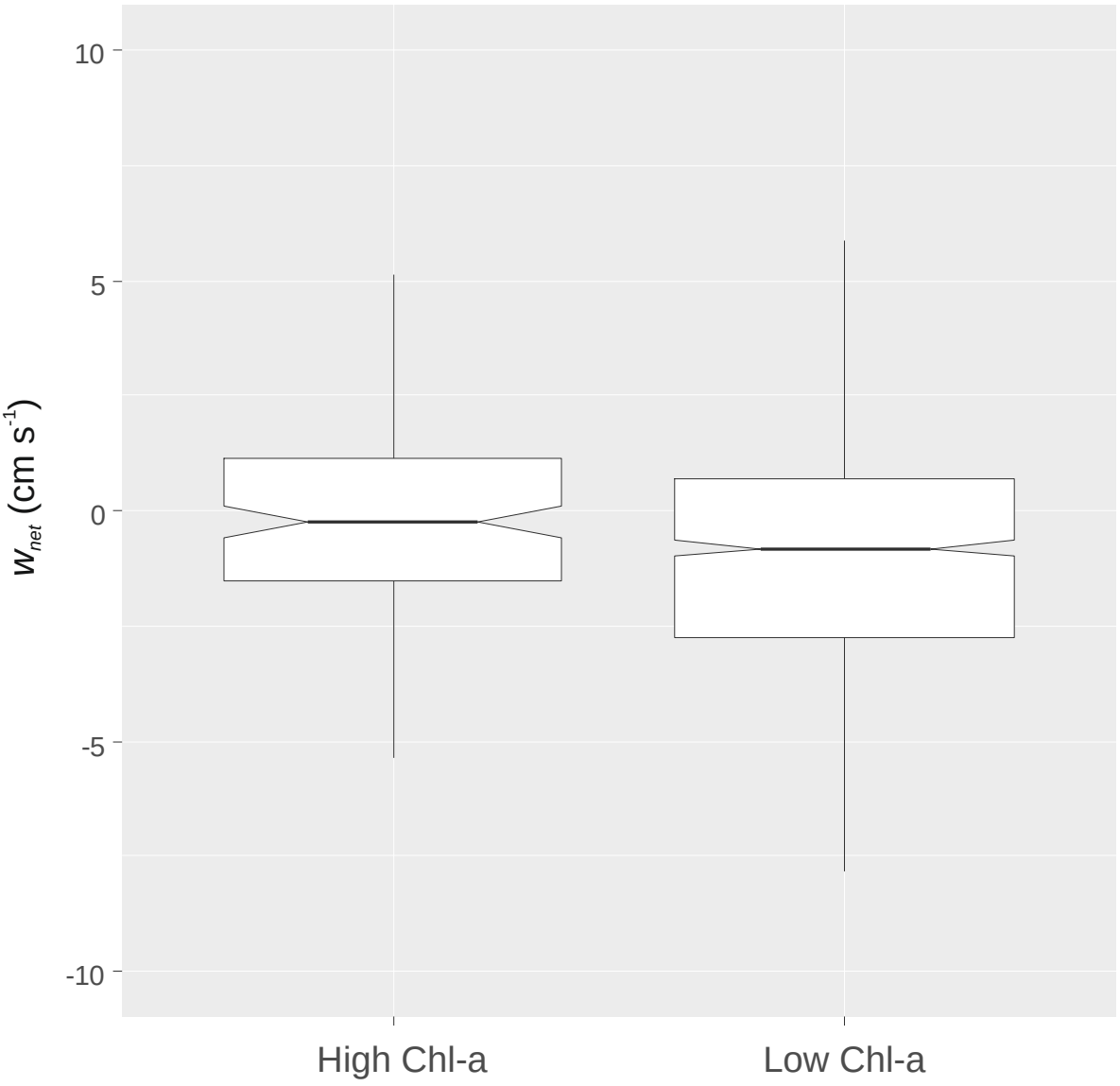
10
5
0
-5
-10
w_{net} (cm s^{-1})
High Chl-a
Low Chl-a

Oceanic swarms of Antarctic krill perform satiation sinking

Geraint A. Tarling, Sally E. Thorpe

British Antarctic Survey, Natural Environment Research Council, High Cross, Madingley Rd, Cambridge, CB3 0ET, UK

Supplementary information

Antarctic krill swarms were analysed from a survey carried out by the *RRS James Clark Ross* between 09 January and 16 February 2003 within the Scotia Sea sector of the Southern Ocean (Cruise JR82, Fig S1). The survey encompassed eight transects within an area of around 30° longitude and 10° latitude and covered a total length of approximately 13000 km. The majority of transects were transited at speeds of 9–18 km h^{-1}. Transect paths crossed a number of oceanographic features such as fronts and eddies as well as open ocean and shelf regions. Acoustic data to detect krill swarms and measure their instantaneous movement were collected using a combination of a calibrated Simrad split-beam EK60 echosounder with 38 kHz and 120 kHz transducers and an RD Instruments narrow-band 153.6 kHz ship-mounted ADCP. Descriptions of how these instruments were set up and operated and the subsequent matching of the data streams are provided in more detail below. Net deployments were made intermittently along the transects from which krill population structure was determined and used for the parameterization of target strength models, as detailed in Tarling et al. [1]

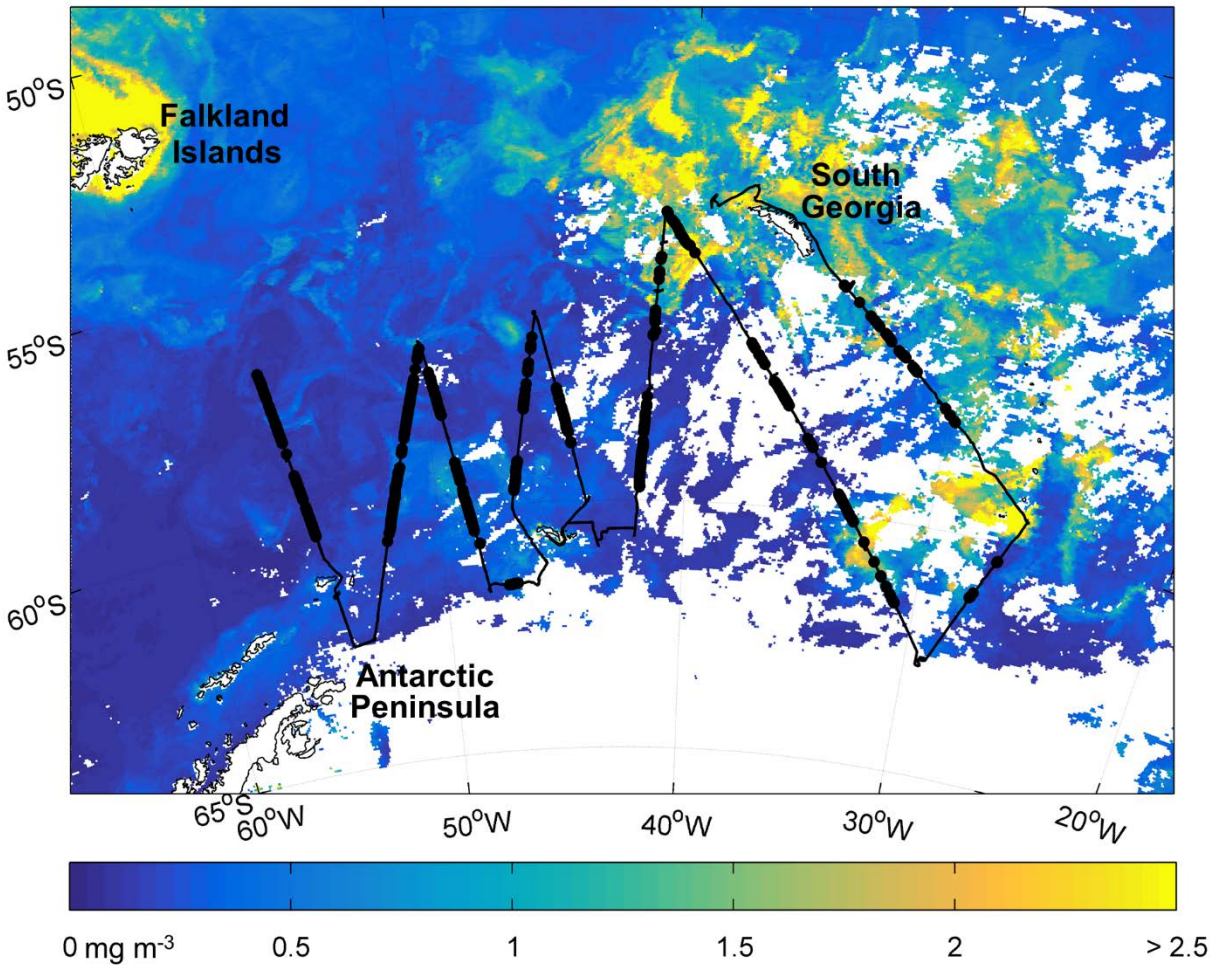

Fig. S1: Mean chlorophyll a (mg m^{-3}) measured by MODIS in the Scotia Sea, 9 January—9 February 2003, 4 km resolution. White areas show missing data due to land, cloud or sea ice. Black line shows the subsection of the JR82 cruise track where swarms were actively being searched for. Black circles show the location of swarms used in this study.

Swarm identification Raw acoustic data from pre-calibrated 38 kHz and 120 kHz transducers were processed using Sonardata Echoview version 4.1 following the protocol of Hewitt et al. [2], and with background noise levels subtracted [3] and bad-data regions filtered out. A threshold of -70 dB at 120 kHz was set following Lawson et al. [4]. A swarm detection algorithm was applied to the processed 120 kHz echogram data using Sonardata Echoview version 4.0 "School detection module", which uses a shoal analysis and patch estimation system algorithm [5] to identify swarm candidates according to preset criteria. In this instance, minimum total swarm length was set to 15 m, minimum distance between

candidates 75 cm, minimum total swarm height 2 m, maximum horizontal linking distance 15 m, and maximum vertical linking distance 5 m. After the swarm-detection process, both 38 and 120 kHz data were exported for interrogation by the Δ_{Sv}120-38 identification technique [6] to identify which swarms contained exclusively Antarctic krill. Minimum and maximum S_v120-38 values for different size ranges of krill were identified from morphometric measurements on samples obtained from accompanying net catches [1]. The parameters were fed into a simplified stochastic distorted wave-borne approximation (SDWBA) target strength model [7-9], using fixed values for orientation of 11° (standard deviation = 4°) and a distribution drawn from 99% of the krill length frequencies estimated from a cumulative distribution function, binned into ranges recommended by Commission for the Conservation of Antarctic Marine Living Resources [6]. The material properties of krill were based on those calculated for the CCAMLR synoptic survey in the Scotia Sea region at the same time of year as the present study [9]. Any swarms that were detected within 100 km of any coastline were excluded from the analysis to ensure that the study only considered the open-ocean situation and not influenced by different behavioural strategies adopted by krill in inshore environments[10].

Measurement of vertical velocity An RD Instruments narrow-band 153.6 kHz ship-mounted ADCP was used to collect underway measurements of vertical velocity (w, cm s^{-1}). The ADCP was in a "janus" configuration, i.e., with two beams looking forward and two looking back at an angle of 30° from vertical in 90° azimuth increments. The firmware version was 17.07, and the data acquisition software, RD Instruments version 2.48. The ensemble period was set to 2 min at a ping rate of 1 Hz, resulting in approximately 120 pings per ensemble. Depth bins were set to 8 m and the blank after transmit, 4 m. The centre of the first bin was set to a depth of 18 m with a total of 64 depth bins being collected per ensemble. All

measurements with % good values of less than 50 were screened out from any further analyses of *w*.

Determining background vertical water movement To determine the net vertical velocity resulting from the presence of a swarm (w_{net}), the background vertical movement of the surrounding water must first be accounted for. We used the average of the ADCP bins immediately above and below each swarm (w_{pre}) to predict this background flow. In all cases, the closest bin above and below the swarm's vertical extent at the mid-length point of the swarm was chosen since this allowed all sizes of swarms to be measured on a similar basis. In some cases, only either the bin above or the bin below provided a valid measurement of background flow since the other measurement was violated by the presence of another swarm or because the swarm was within the shallowest depth bin measured by the ADCP.

Simulation data sets were generated to identify any bias in the prediction of background flows within a swarm based on w_{pre}. Locations were selected at random along the cruise track (N = 2980, representing all identified krill swarms for which a vertical velocity measurement was also available). All locations containing krill swarms were rejected. For each of the remaining locations, swarms were simulated through randomly selecting swarm-depth, -thickness and -length values from the observed distributions of these parameters (Table S1) and then using these to define the region of a "fake" swarm (denoted *f* as opposed to an observed swarm, denoted *s*). $w_{pre,f}$ was compared with the observed vertical flow within the fake swarm ($w_{obs,f}$) to establish whether any biases or artefacts were apparent. No significant difference was found between the predicted and the observed vertical velocities (median $w_{pre,f}$ 2.44 cm s^{-1}, median $w_{obs,f}$ 2.53 cm s^{-1}, Mann-Whitney [MW] rank sum test U = 4439200, T = 8880890, n(small, big) = 2980, P = 0.988, following a failed Kolmogorov-Smirnov test for normality). Accordingly, the net influence that krill have on vertical velocities within the body of the swarm (w_{net}) can be estimated by subtracting $w_{pre,s}$ from the vertical velocities

observed within the swarm ($w_{obs,s}$). We otherwise term w_{net} as the vertical velocity anomaly. The total number of swarms for which there was a valid estimate of both $w_{pre,s}$ and $w_{obs,s}$ from which to determine w_{net} was 2043. Vertical velocity within swarms ($w_{obs,s}$) was significantly lower than that of the bins above and below ($w_{pre,s}$, MW test, U = 1840070, T = 3928016, n(small, big) = 2043, P = <0.001). Median $w_{obs,s}$ was 1.43 cm s^{-1}, compared with the median $w_{pre,s}$ of 2.22 cm s^{-1}. The median vertical velocity anomaly within swarms ($w_{net} = w_{obs,s} - w_{pre,s}$) was -0.61 cm s^{-1} (a negative value denoting a downward velocity).

Dataset	N	Depth (m)	Length (m)	Thickness (m)	Surface Chl-a (mg m^{-3})	Acoustic backscatter (S_v in dB)	Target strength (dB)	Packing conc. (ind m^{-3})	$w_{obs,s}$ (cm s^{-1})	$w_{pre,s}$ (cm s^{-1})	w_{net} (cm s^{-1})
All	2043	38.13 (28.63, 54.57)	41.51 (25.74, 80.05)	4.62 (2.58, 8.71)	0.23 (0.18, 0.34)	-64.71 (-66.56, -61.21)	-74.57 (-74.64, -74.49)	9.68 (6.26, 21.85)	1.43 (-1.82, 3.97)	2.22 (-0.41, 4.80)	-0.61 (-2.43, 1.01)
Day	1802	37.05 (28.13, 51.19)	41.96 (25.78, 86.27)	4.81 (2.58, 8.90)	0.23 (0.18, 0.33)	-64.55 (-66.46, -61.22)	-74.57 (-74.64, -74.49)	10.01 (6.43, 21.71)	1.11 (-2.23, 3.96)	2.14 (-0.71, 4.88)	-0.71 (-2.74, 1.01)
Dusk	31	95.42 (37.57, 125.25)	31.44 (21.66, 47.05)	3.51 (2.39, 4.62)	0.19 (0.13, 0.19)	-65.79 (-67.16, -57.06)	-74.48 (-74.57, -74.48)	7.40 (5.41, 56.30)	1.42 (0.15, 2.69)	1.06 (-0.35, 3.04)	-0.10 (-1.01, 1.14)
Night	163	64.28 (33.69, 117.93)	38.34 (25.64, 55.95)	4.25 (2.30, 7.60)	1.10 (0.95, 1.84)	-66.52 (-67.35, -64.70)	-74.49 (-74.49, -74.49)	6.39 (5.27, 9.82)	2.12 (0.91, 3.03)	2.22 (0.83, 3.26)	-0.10 (-0.91, 0.81)
Dawn	47	61.52 (39.98, 86.89)	39.09 (27.14, 47.07)	4.81 (3.14, 7.50)	0.32 (0.24, 1.84)	-63.68 (-66.44, -56.10)	-74.49 (-74.64, -74.49)	12.35 (6.38, 69.07)	5.57 (3.70, 9.39)	5.25 (2.82, 8.81)	0.50 (-0.65, 1.85)
<0.5 mg m^{-3} sea surface Chl-a	921	38.90 (29.22, 53.36)	41.41 (25.84, 80.76)	5.37 (2.95, 9.83)	0.22 (0.17, 0.28)	-63.81 (-66.03, -59.82)	-74.64 (-74.64, -74.49)	12.02 (7.11, 30.33)	1.52 (-1.55, 4.26)	2.40 (-0.10, 5.21)	-0.81 (-2.74, 0.71)
≥0.5 mg m^{-3} sea surface Chl-a	149	43.69 (25.83, 90.97)	47.66 (27.70, 76.19)	4.06 (2.21, 7.22)	0.83 (0.57, 1.17)	-65.88 (-67.00, -63.78)	-74.49 (-74.49, -74.49)	7.40 (5.62, 11.19)	1.51 (0.10, 2.83)	2.32 (0.71, 3.69)	-0.25 (-1.52, 1.16)
<0.5 mg m^{-3} sea surface Chl-a (day only)	873	38.74 (29.05, 52.79)	41.71 (26.20, 82.65)	5.37 (2.95, 10.01)	0.22 (0.17, 0.28)	-63.84 (-65.97, -60.04)	-74.64 (-74.64, -74.49)	11.98 (7.26, 28.69)	1.47 (-1.82, 4.17)	2.34 (-0.30, 5.27)	-0.81 (-2.84, 0.71)
≥0.5 mg m^{-3} sea surface Chl-a (day only)	103	35.30 (22.82, 47.20)	47.18 (22.58, 82.32)	3.69 (2.02, 7.88)	0.70 (0.57, 0.86)	-65.09 (-66.78, -62.32)	-74.49 (-74.64, -74.49)	8.70 (5.95, 16.63)	1.32 (-1.22, 4.25)	2.57 (-0.10, 4.54)	-0.30 (-1.73, 1.52)

Table S1: Swarm properties from cruise JR82 (January—February 2003) in relation to time of day and levels of surface Chl-a. Values represent medians with 25th and 75th centiles in brackets.

Statistical analyses To test for differences in the distribution of w_{net} at different times of day, the dataset was divided accordingly: day – 06:00-00:59 hrs GMT, dusk – 01:00-01:59 hrs GMT, night – 02:00-04:59 hrs GMT, dawn – 05:00-05:59 hrs GMT (Nb: local midday was at 15:00 hrs GMT, local midnight – 03:00 hrs GMT). These datasets were not normally distributed (both failed a Shapiro-Wilk test for normality) so the significance of differences was determined through a Kruskal-Wallis One Way Analysis of Variance on Ranks. This was followed by an All Pairwise Multiple Comparison Procedure using Dunn's Method to determine which individual comparisons were significantly different. We found there to be a significant difference in w_{net} between different phases of the diel cycle (Krusall-Wallis 1-way ANOVA, H = 29.98, 3 df, P<0.001, Fig. 4). Individual significant difference were found between day and night (All pairwise comparison, Dunns Method, difference in ranks 183.1, Q = 3.794), and between dawn and day (Difference in ranks 327.4, Q = 3.757). All other comparisons did not show significant differences. Daytime contained the lowest median value for w_{net} (-0.71 cm s^{-1}) with nighttime and dusk also exhibiting negative median vertical velocity anomalies (both being -0.10 cm s^{-1}). w_{net} was positive during dawn (0.51 cm s^{-1}).

To determine the influence of the biomass of phytoplankton on w_{net}, swarms were matched to the relevant spatial 4 x 4 km pixel of 8-day synthesised sea surface chlorophyll-a (Chl-a) images provided by the MODIS instrument on board the Aqua satellite (operated by NASA). Swarms were found at Chl-a values between 0 and 3.31 mg Chl-a m^{-3}, with a median value of 0.26 mg Chl-a m^{-3} and a mean of 0.34 mg Chl-a m^{-3}. A region of high Chl-a was categorised as containing values at or above 0.5 mg Chl-a m^{-3}, with the remainder categorised as low Chl-a. The significance level of the difference in w_{net} between regions of high and low Chl-a was tested in two scenarios, one including all times of day and night and the other, daytime only. An MW test was used for both tests, following a failed prior Shapiro-Wilk test for normality. w_{net} was significantly more negative in regions with low levels of surface Chl-a compared to

regions where surface Chl-a was high, both when including all times of day and night (MW test, U = 59654, T = 88409 n(small)= 150, n(big)= 913, P = 0.007) and when restricting the analysis to daytime only (MW test, U = 39204, T = 55969, n(small)= 103, n(big)= 872, P = 0.035). Across all times of day and night, median w_{net} was -0.81 cm s^{-1} in low Chl-a conditions compared to -0.31 cm s^{-1} when Chl-a was high

The effect of light on swarm behaviour was tested through matching observed swarms with photosynthetically active radiation (PAR), measured by a parlite quantum sensor (Kipp and Zonen) onboard the ship, which collected measurements at 5 s intervals, subsequently averaged into 1 min intervals. Swarms resolved during daylight hours were divided into high PAR (> 500 W m^{-2}) and low PAR (100 to 500 W m^{-2}) groups and an MW test was performed to determine if PAR during the daytime had a significant influence on w_{net}. During the daytime, we found no influence of different levels of daylight on w_{net} when comparing between low PAR and high PAR situations (MW test, U = 19909, T = 379208, n(small) = 588, n(big) = 689, P = 0.597).

References

[1] Tarling, G.A., Klevjer, T., Fielding, S., Watkins, J., Atkinson, A., Murphy, E., Korb, R., Whitehouse, M. & Leaper, R. 2009 Variability and predictability of Antarctic krill swarm structure. *Deep-Sea Res. Part II* **56**, 1994-2012. (doi:10.1016/j.dsr.2009.07.004).

[2] Hewitt, R.P., Kim, S., Naganobu, M., Gutierrez, M., Kang, D., Takao, Y., Quinones, J., Lee, Y.H., Shin, H.C., Kawaguchi, S., et al. 2004 Variation in the biomass density and demography of Antarctic krill in the vicinity of the South Shetland Islands during the 1999/2000 austral summer. *Deep-Sea Res. Part II* **51**, 1411-1419. (doi:10.1016/j.dsr2.2004.06.018).

[3] Watkins, J.L. & Brierly, A.S. 1996 A post processing technique to remove background noise from echo-integration data. *J. Mar. Sci.* **53**, 339-344. (doi:10.1006/jmsc.1996.0046).

[4] Lawson, G.L., Wiebe, P.H., Ashjian, C.J. & Stanton, T.K. 2008 Euphausiid distribution along the Western Antarctic Peninsula - Part B: Distribution of euphausiid aggregations and biomass, and associations with environmental features. *Deep-Sea Res. Part II* **55**, 432-454. (doi:10.1016/j.dsr2.2007.11.014).

[5] Coetzee, J. 2000 Use of a shoal analysis and patch estimation system (SHAPES) to characterize sardine schools. *Aquat. Liv. Res.* **13**, 1-10. (doi:10.1016/S0990-7440(00)00139-X).

[6] CCAMLR. 2005 Report of the first meeting of the subgroup on acoustic survey and analysis methods *SC-CCAMLR-XXIV/BG/3*.

[7] McGehee, D.E., O'Driscoll, R.L. & Traykovski, L.V.M. 1998 Effects of orientation on acoustic scattering from Antarctic krill at 120 kHz. *Deep-Sea Res. Part II* **45**, 1273-1294. (doi:10.1016/S0967-0645(98)00036-8).

[8] Demer, D.A. & Conti, S.G. 2003 Reconciling theoretical versus empirical target strengths of krill: effects of phase variability on the distorted- wave Born approximation. *ICES J. Mar. Sci.* **60**, 429-434. (doi:10.1016/S1054-3139(03)00002-X).

[9] Conti, S.G. & Demer, D.A. 2006 Improved parameterization of the SDWBA for estimating krill target strength. *ICES J. Mar. Sci.* **63**, 928-935. (doi:10.1016/j.icesjms.2006.02.007).

[10] Klevjer, T.A., Tarling, G.A. & Fielding, S. 2010 Swarm characteristics of Antarctic krill Euphausia superba relative to the proximity of land during summer in the Scotia Sea. *Marine Ecology Progress Series* **409**, 157-170. (doi:10.3354/meps08602).